Steady-state kinetics of alpha-synuclein ferrireductase activity identifies the catalytically competent species.

Jennifer S. McDowall, Ioanna Ntai, Jonathon Hake, Paul R. Whitley, Jody M. Mason, Christopher R. Pudney* and David R Brown*

Department of Biology and Biochemistry, Faculty of Science, University of Bath, Bath, UK.

Short Title: Alpha-synuclein ferrireductase is an oligomer

Key words: synuclein, oligomer, ferrireductase, Parkinson's disease

* Co-corresponding authors. C.R.Pudney@bath.ac.uk. D.R.Brown@bath.ac.uk

Abstract

α-syn is a cytosolic protein known for its association with neurodegenerative diseases that include Parkinson's disease and other synucleinopathies. The potential cellular function of α-synuclein may be of consequence for understanding the pathogenesis of such diseases. Previous work has suggested that α-synuclein can catalyse the reduction of iron as a ferrireductase. We performed a detailed analysis of the steady-state kinetics of recombinant α-syn ferrireductase activity and for disease associated variants. Our study illustrates that the ferrireductase activity we observed is clearly commensurate with *bone fide* enzyme activity and suggest a mechanistic rationale for the activity and the relationship to cellular regulation of the pool of Fe(III)/ Fe(II). Using cell based studies we examined the functionally active conformation and found that the major catalytically active form is a putative membrane associated tetramer. Using an artificial membrane environment with recombinant protein, we demonstrate that secondary structure folding of α-synuclein is insufficient to allow enzyme activity and the absolute specificity of the tertiary/quaternary structure is the primary requirement. Finally, we explored the steady-state kinetics of a range of disease α-synuclein variants and found that variants involved in neurodegenerative disease exhibited major changes to their enzymatic activity. We discuss these data in the context of a potential disease associated mechanism for aberrant α-synuclein ferrireductase activity.

Introduction

Alpha-synuclein (α-syn) is a member of a family of proteins termed the synucleins[1, 2]. It has been associated with a range of neurodegenerative diseases unified under the name of synucleinopathies, chief of which is Parkinson's disease (PD) [3, 4]. Other synuclein family members include β-synuclein (β-syn) and γ-synuclein. α-syn and β-syn are co-localised in neurons[5], but α-syn has gained more attention, because of its potential to aggregate and form Lewy Bodies that are seen in the synucleinopathies [6]. α-syn is a 14 kD protein that has been most commonly described as a monomeric, unstructured protein of the cytosol. However, there is considerable evidence that it can associate with the plasma membrane and gain helical content [7-10]. There is also evidence suggesting that some amount of the cellular form can form tetramers that are rich in helical content[11]. The function of α-syn in cells remains unclear. Knockout of the protein in transgenic mouse lines does not alter viability or brain architecture, but has mild effects on dopamine release [12]. There are some reports that α-syn knockout alters behaviour[13].

Various molecular studies have suggested a range of functions for α-syn. As the protein is expressed in dopaminergic neurons, it has been suggested that the protein regulates dopamine release[14]. Particularly, α-syn is thought to be involved in SNARE dependent vesicle fusion leading to neurotransmitter release [15]. This is supported by studies that suggest α-syn is localised to the presynaptic terminals[16], but α-syn has also been found in the nucleus. In this case it has been suggested to have a role in gene transcription via inhibiting histone acetylation[17]. Other studies have suggested that α-syn is localised to the mitochondria, where it may be involved in mitochondrial function [18]. α-syn has been suggested to bind metals including copper and iron. In this regard, α-syn has been suggested to catalyse the reduction of iron[19].

Ferrireductase (FR) activity in cells is vital to ensure the availability of Fe(II) for a range of cellular processes and particularly those enzymatic activities that require Fe(II) as a co-factor. In dopaminergic neurons, such as those in the substantia nigra, lost during that pathogenic advance of PD, Fe(II) is required as a co-factor for tyrosine hydroxylase involved in the synthesis of dopamine[20]. PD is also associated with disturbances in brain iron homeostasis [21, 22]. Recently, it has been suggested that α-syn can act as a ferrireductase[19]. Therefore, α-syn, which is highly expressed in the substantia nigra, could serve a role in the regulation of the balance of Fe(II) to Fe(III) in this key region.

The previous evidence for the enzymatic activity of α-syn has come from studies with purified recombinant protein from bacterial sources and some studies of α-syn expressed in mammalian cells[19]. Overexpression of α-syn in cells elevated the level of Fe(II) present. While this evidence allowed us to demonstrate the FR activity, it did not provide evidence of the active species of the protein or which domains are necessary for its activity. Such information is of great interest given the recent identification of a tetrameric form of α-syn which has been suggested to be of great importance to understanding the protein's normal role in cells. In this article we provide more complete evidence for the enzymatic role of α-syn in iron reduction and provide evidence that the active form is a membrane associate species that is either a dimer or a tetramer.

Materials and methods

Reagents were purchased from Sigma-Aldrich (Poole, UK) unless otherwise stated.

Purification of synuclein proteins. Using pET expression vectors in BL21 *E. coli* cells, untagged α-syn protein expression was induced at OD_{600} 0.5 – 1.0 with 1 mM IPTG for 4 hours. Cells were harvested by centrifugation (8000 x *g*) and lysed mechanically in 20 mM Tris-HCl/1 mM EDTA/pH 8.0 (Buffer A), 1 mM PMSF and 50 µg/mL DNase. Streptomycin sulfate was added to a final concentration of 1% to the lysate solution then centrifuged at 8000 x g. Ammonium sulfate (0.295 g/mL) was added to the supernatant (15% w/v solution) and stirred at 4 ºC for at least 1 hour. After centrifugation at 10,000 x g, the pellet was resuspended 50 mL Buffer A. The semi-purified lysate solution was loaded onto a 10 mL Q Sepharose column (Amersham Biosciences). The column was washed with 100ml Buffer A, then 2 column volume isocratic elution step to 25% Buffer A + 1 M NaCl (Buffer B). Synuclein proteins were eluted with a broad gradient elution (10 column volumes) from 25% Buffer B to 50% Buffer B (all synuclein proteins eluting at approximately 350 mM NaCl). SDS-PAGE analysis of Q Sepharose fractions was performed and fractions enriched for synuclein were pooled. Synuclein proteins were collected as flow through from a PM30 cellulose membrane (Millpore) then concentrated with a PM10 PES membrane (Millipore). Purified synuclein proteins were dialysed extensively at 4 ºC in chelex-treated MilliQ. Protein Concentration was measured by absorbance at 275nm with extinction coefficient of 5600 $M^{-1}cm^{-1}$. Mutants of wild-type α-syn were as previously described[23]. Purity of the recombinant protein was confirmed through samples sent to the Mass Spectroscopy Facility at the University of Bristol. Examples of protein purification are included in the supplementary material (Suppl.

Figure 1)

Cell culture. SH-SY5Y (human neuroblastoma) cells were cultured in 45% DMEM/45% Ham's F12 supplemented with 10% FBS, and 1% pen/strep. Cells were maintained at 37ºC and 5% CO_2 in a

humidified incubator. The neuronal status of SH-SY5Y cells was monitored by RT-PCR with primers for tyrosine hydroxylase (TH), dopamine transporter (DAT) and vesicle mono-amine transporter 2 (VMAT2). Cells were used within 20 passages of the original vial.

Ferrireductase Assay. The ferrireductase activity was measured essentially as previously described [19], monitoring the concentration dependence of β-nicotinamide adenine dinucleotide hydride (NADH) and ferric ammonium citrate [Fe (III)]. For cell-based assays, cells were grown to 90% confluence and the flask of cells scraped into distilled water and centrifuged immediately at 13k r.p.m. The resulting membrane pellets were then washed in PBS three times with subsequence centrifugation. The final pellet was the resuspended in PBS with 1% Igepal and incubated on ice for 20 minutes. The extract was then cleared of debris by centrifugation and the supernatant used for experiments. The protein concentration was determined using a standard Bradford Assay (Biorad) and applied to the ferrireductase assay. The cell-based assay used 20 mM MOPS pH 7, 500 μM NADH, 500 μM ferrozine and 250 μg/ml of the test protein.

Stopped-flow fluorescence, circular dichroism and dynamic light scattering measurements. Absorbance changes were monitored on a thermostated Hi-Tech Scientific stopped-flow apparatus (TgK Scientific, Bradford on Avon, UK). Typically 3 - 5 transients were recorded for each reported measurement. Transients were fit as described in the text. Circular dichroism measurements were made on a thermostated Applied Photophysics Chirascan spectrophotometer (Applied Photophysics, Leatherhead, UK) using a high-quality quartz cell with a 0.1 mM path length. Dynamic light scattering (DLS) profiles were recorded using a Malvern Zetasizer DLS incubated at 25 °C recorded as percent volume.

Nanodisc preparation. L-α-phosphatidylcholine from soybean (sigma P3644-25G) was resuspended in 20 mM Hepes pH 7.5 100 mM NaCl to give a 10 mM suspension of liposomes. This suspension was

extruded for 15 passes through a 100 nm membrane (Sigma, WHA800309) using a mini extruder (Avanti Polar Lipids). Hydrolysed SMA polymer (3:1 ratio of styrene:maleic acid) was a gift from Professor Karen Edler (Dept. of Chemistry, University of Bath). The polymer was solubilised in 20 mM Hepes pH 7.5 100 mM NaCl at 6% w/v. For preparation of nanodiscs a 1:3 ratio of 6% w/v SMA: 10 mM extruded liposomes was incubated at 18^{o}C for 2 hours. Nanodiscs preparations (1.5% w/v SMA, 7.5 mM lipid) were analysed by dynamic light scattering (DLS) for quality control. We note that the size of the nanodiscs as assessed by DLS corresponds with previous reports based on NMR studies (see below).

Results

α-syn is a bone fide ferri-reductase. We used an established assay for detecting the formation of Fe(II), based on the optical absorption of 3-(2-pyridyl)-5,6- bis(phenyl sulfonic acid)-1,2,4-tri-azine (ferrozine) at 562 nm, which increases upon binding of Fe(II). The assay is highly specific for the presence of Fe(II) with essentially no change in the presence of Fe(III). This indirect assay has the potential to be a confounding factor in the analysis of ferri-reductase activity. That is, if the rate of Fe(II) binding to ferrozine is slow, or at least slower than the activity of the enzyme, then Fe(II) binding becomes the rate limiting step. We have therefore monitored the rate of Fe(II) binding to ferrozine, assessed by the absorption change at 562 nm in a stopped-flow apparatus. An example stopped-flow transient is shown in Figure 1A. The data fit to a single exponential function:

$$\Delta A_{obs} = A \exp(-k_{obs}t) \qquad \text{Eq 1}$$

Where ΔA_{obs} is the change in the observed absorption of ferrozine with respect to time (t), A is the amplitude of the kinetic transient giving an observed rate constant (k_{obs}).

That the data fit to a single exponential suggests only a single physical step in the binding interaction. The observed rate extracted from Eq 1 is $k_{obs} = 12.29 \pm 0.1\ s^{-1}$. The observed rate of Fe(III) binding to ferrozine is therefore at least three orders of magnitude faster than the values of k_{cat} we observe for α-syn (*vida infra*) and so, at least for α-syn, the assay reflects enzyme turnover and Fe(II) formation. We cannot comment on the mechanistic step or steps we access with this assay however, other than it most likely reflects the slowest step in the turnover of Fe(III) to Fe(II).

The key experimental test for enzyme activity is the observation of a linear relationship between the observed rate of turnover and the enzyme concentration. Figure 1B shows the concentration

dependence of α-syn on the observed rate of Fe(II) formation. We found that the data fit to a simple linear function that intersects both axes essentially at zero. That is, the rate of Fe(II) formation increases linearly with the concentration of α-syn, suggesting that the observed ferri-reductase reaction is truly enzyme catalysed by α-syn. As an additional step of verification we compared α-syn ferriductase activity with and without boiling of the protein. Boiling of the protein for 1 h completely inactivates the protein (Suppl. Figure 2).

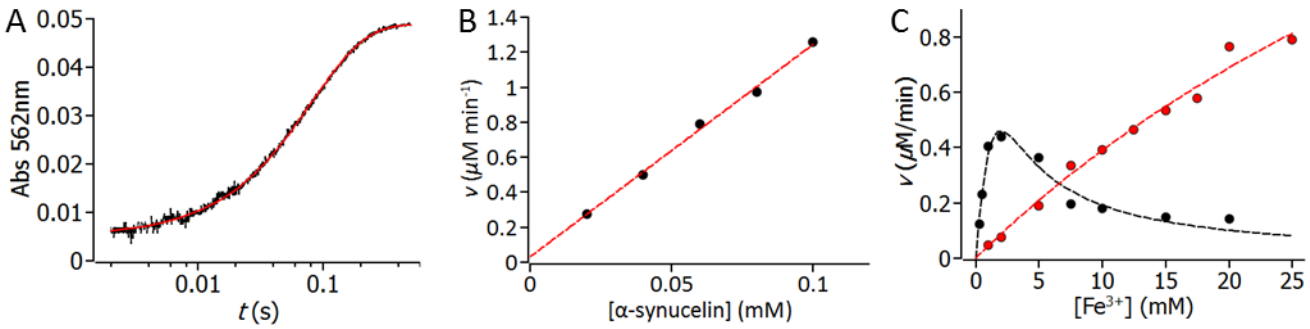

Figure 1. A, Characterisation of the assay used to detect ferrireductase activity. Stopped-flow kinetics monitoring the increase in absorbance at 562 nm upon rapid mixing of 10 μM Fe (II) with Ferrozine. The red line is the fit to a single exponential function. **B,** Steady-state kinetics monitoring the formation of Fe(II) in the presence of increasing concentration α-syn. The red dashed line is the fit to a linear function. **C,** Steady-state kinetics of α-syn monitoring the formation of Fe(II) as a function of increase NADH (red) and Fe(III) (black) concentration. Solid lines are fits to Eq 2 (red) and Eq 3 (black).

Figure 1C shows the concentration dependence of Fe(III) and NADH on the rate of Fe(II) formation in the presence of 100 μM α-syn. For NADH, we found that the data can be adequately fitted to the

Michaelis-Menten equation, giving values of k_{cat} = 2.93 ± 0.95 (10^{-2}) min^{-1} and K_m = 65.2 ± 26.9 mM. For Fe(III), the data do not fit to a simple Michaelis-Menten relationship (Eq 2) but instead show an initial increase on observed rate and then a decrease at higher Fe (III) concentrations. The data fit to a model that includes substrate inhibition (Eq 3),

$$v = \frac{k_{cat}[E]_0[S]}{K_m+[S]} \qquad \text{Eq 2}$$

$$v = \frac{k_{cat}[E]_0[S]}{K_m+[S]\left(\frac{1+[S]}{K_i}\right)} \qquad \text{Eq 3}$$

Where K_i is an inhibition constant. Fitting the data to Eq 3 gives, k_{cat} = 3.66 ± 4.9 (10^{-2}) min^{-1}, K_m = 7.0 ± 10.5 mM and K_i = 0.57 ± 0.85. The magnitude of k_{cat} is relatively small. This could point to either a high barrier to transition-state formation, a very slow rate-limiting step in the overall enzymatic turnover (including substrate binding, chemical turnover and product release) or a small fraction of the total protein being in a catalytically competent conformation. The observation of a large K_m value in the mM region for both NADH and Fe (III) suggests the ternary *reactive* complex is weakly bound.

For such a two-substrate system, one would like to make the steady-state measurements at a saturating concentration of one substrate. This is not possible in the present case since the K_M^{app} values are large and to saturate these would place the concetrations beyond the solubility limits of the substrates. We therefore prefer to interpret the relative trends in our data rather than the absolute magnitudes.

α-syn variants suggest a pathological link to ferri-reductase activity. We explored the Stead-state kinetics of a range of key, pathologically relevant α-syn variants shown in Figure 2A and 2B with the resulting extracted values from the fits given in Table 1. Figure 2C shows a summary of our findings with respect to the structural location of the α-syn variants.

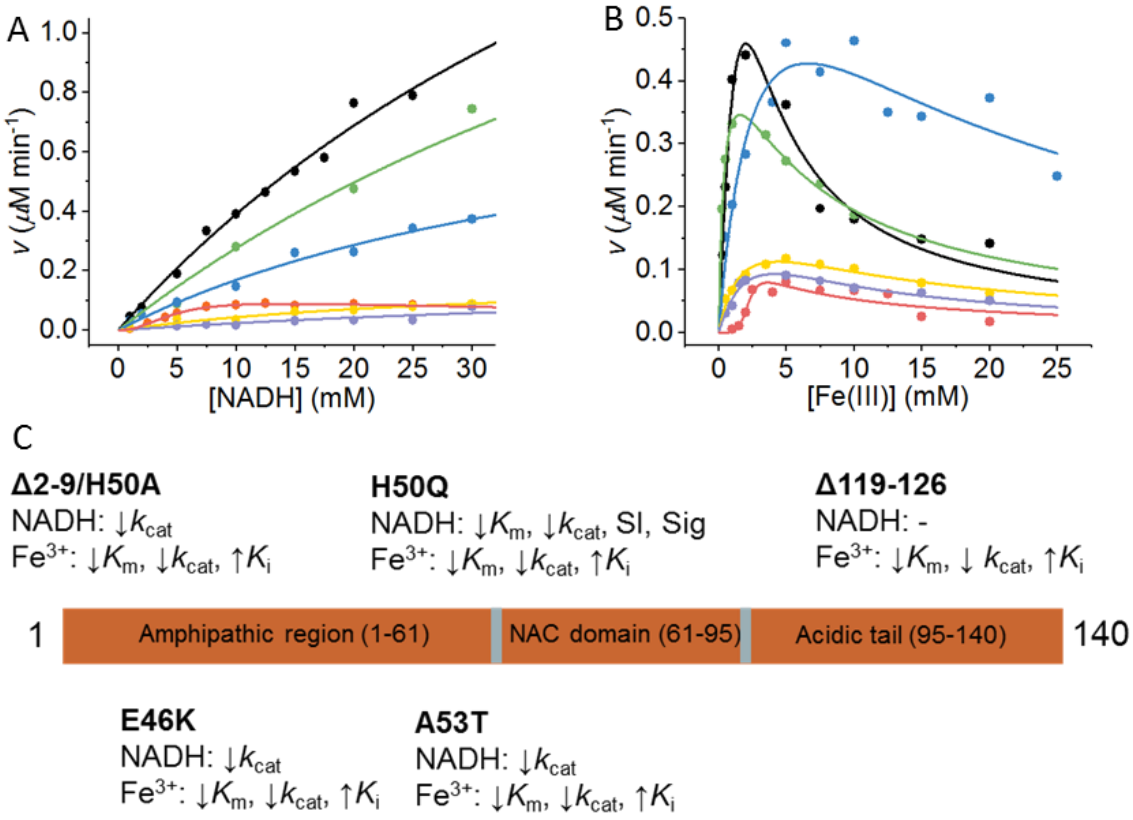

Figure 2. Steady-state kinetics of α-syn showing concentration dependencies with NADH (Panel A) and Fe^{3+} (Panel B). Solid lines are fits to models described in Table 1, with the corresponding extracted parameters. Wild-type synuclein (black), H50Q (coral), A53T (blue), E46K (yellow), Δ119-126 (green), Δ2-9/H50A (lilac). **C,** Summary of the effect of different variants on the steady-state kinetics of α-syn.

Table 1. Extracted parameters from steady-state data fitting shown in Figure 2.

	V_{max}^{app} (μM/min)	K_M^{app} (mM)	k_{cat}^{app} (min^{-1})	k_{cat}^{app}/K_M^{app} (min^{-1} mM^{-1})	K_i^{app} (mM)	n
[NADH] - dependence						
α-syn[a]	2.93 ± 0.95	65.2 ± 26.9	2.93 × 10^{-2}	4.50 × 10^{-4}	-	-
Δ119-126	2.5 ± 0.7	80.9 ± 32.8	2.5 × 10^{-2}	3.1 × 10^{-4}	-	-
H50Q[b]	0.12 ± 0.02	5.0 ± 0.8	0.12 × 10^{-2}	2.4 × 10^{-4}	63.3 ± 40.0	2.1 ± 0.3
A53T	0.94 ± 0.24	45.6 ± 17.5	0.94 × 10^{-2}	2.0 × 10^{-4}	-	-
E46K	0.19 ± 0.03	32.9 ± 10.4	0.19 × 10^{-2}	5.7 × 10^{-5}	-	-
Δ2-9/H50A	0.20 ± 0.15	73.6 ± 82.5	0.20 × 10^{-2}	2.7 × 10^{-5}	-	-
[Fe^{3+}] - dependence						
α-syn[c]	3.66 ± 4.9	7.0 ± 10.5	3.66 × 10^{-2}	5.2 × 10^{-3}	0.57 ± 0.85	-
Δ119-126	0.55 ± 0.02	0.46 ± 0.1	0.55× 10^{-2}	1.12 × 10^{-2}	5.43 ± 0.53	-
H50Q[b]	0.13 ± 0.06	2.3 ± 0.4	0.13 × 10^{-2}	6 × 10^{-6}	7.1 ± 5.8	5.4 ± 3.0

A53T	0.84 ± 0.24	3.14 ± 1.6	0.84×10^{-2}	2.7×10^{-5}	13.8 ± 7.5	-
E46K	0.21 ± 0.03	1.9 ± 0.57	0.21×10^{-2}	1.1×10^{-6}	10.0 ± 3.1	-
Δ2-9/H50A	0.25 ± 0.1	3.39 ± 1.8	0.25×10^{-2}	7.2×10^{-6}	5.0 ± 2.8	-

a, MM kinetics. b, Substrate inhibition. c, Cooperative binding and substrate inhibition. In all cases the simplest model was selected based on the extraction of realistic fitting parameters and statistical quality of the fit.

(i) A53T and E46K are mutations in the SPCA gene associated with inherited forms of PD**.** The K_m was relatively unaffected for NADH with a decrease for Fe^{3+} but k_{cat} was significantly reduced in both cases. **(ii)** H50Q is a mutation identified from inherited cases of PD. The H50 site could influence metal binding and is associated with increased oligomerisation and fibril formation of α-syn. We find a significantly reduced K_m but also a significantly lower k_{cat} for both NADH and Fe(III). We observed a complex kinetic relationship for both substrates, exhibiting both a sigmoidal relationship, suggestive of cooperatvity, as well as substrate inhibition. We fitted these data to the function:

$$v = \frac{k_{cat}[E]_0[S]^n}{K_m^n + [S]^n + \left(\frac{1+[S]^n}{K_i}\right)} \qquad \text{Eq 4}$$

Such a relationship is paradigmatic of the activity of other enzymes for example aspartate transcarbamylase[24]. These data therefore suggest either induction or unmasking of a cooperative relationship. Potentially these data may indicate that there are multiple discrete binding geometries for both NADH and Fe(III) in the H50Q variant and certainly that this metal binding site is key to the forming the optimal reactive geometry with both substrates. **(iii)** Δ2-9/H50A is a deletion of the N-terminus of the protein that has been shown to be the site of high affinity copper[25] binding and also removes the H50 residue from any potential role in metal binding. The K_m is relatively unaffected for NADH with a decrease for Fe(III) but k_{cat} is significantly reduced in both cases. These data therefore suggest that the N-terminus is not significantly involved in the binding of either NADH or Fe^{3+}, but is

required for full enzymatic activity. Potentially the copper binding increases the propensity to form a catalytically competent conformation. **(iv)** Δ119-126 represents the removal of a potential low affinity divalent metal binding site. The k_{cat} and K_m for NADH are hardly affected by this variant but both the k_{cat} and the K_m are significantly affected for Fe(III). The mutant data suggest this site is not involved in NADH binding or oxidation but is key to reduction and binding of the Fe(III).

Differences in k_{cat} between the mutants could be explained either by different conformational states of the proteins or by a smaller/larger proportion of a catalytically active conformation or alternatively as a consequence specifics of the two-substrate mechanism. However, differences in the equilibrium constants K_m and K_i are not dependent on the proportion of the catalytically active species, but instead on differences in binding geometry, particularly for the reactive complex. That we observe significant changes in k_{cat}, K_m, K_i and the induction of cooperative like behavior (H50Q) argues strongly for structurally different forms of the mutants studied. Crucially this does not rule out a fraction of the recombinant protein being active and we explore this possibility below. We note that we do not suggest that the observed kinetic differences are the sole driver of disease state, since clearly aggregation propensity is a key factor. However, the key finding is that these data demonstrate that these disease variants can significantly alter the kinetics of FR activity.

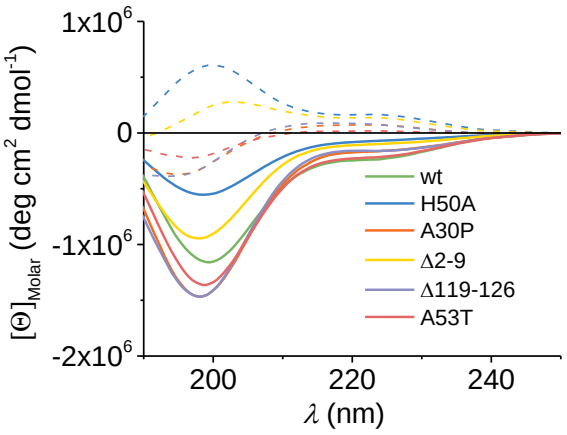

Figure 3. Far-UV CD spectra of recombinant α-syn and variants. Solid lines are spectra corresponding to each variant and the dashed lines are the corresponding difference spectra for each variant with respect to WT α-syn.

CD Analysis We have explored whether there is evidence of α-syn mutant conformational change through comparative far-UV circular dichroism (CD) spectroscopy shown in Figure 3. The Far-UV CD spectra of each mutant, as with WT α-syn, are indicative of a protein with an extremely high degree of unstructured content. However, the spectra show clear differences; the dashed line in Figure 3 shows the difference spectra of each mutant compared to the WT α-syn. In the case of A30P, A53T and Δ119-126 α-syn the difference spectra are extremely characteristic of unstructured content with a negative peak at ~198 nm and a small broad and positive peak at ~220 nm. The difference spectra for H50A and Δ2-9 are complex and do not present an obvious structural interpretation. Far-UV CD data are limited in the ability to quantitatively interpret unstructured content. However, our data suggest there is at least some conformational difference arising from the mutations studied. These data therefore provide a rationale for the different equilibrium constants, suggesting that the mutant structures affect the formation of the reactive ternary complex and potentially part of the differences in the extracted k_{cat} values. The absolute magnitude of the k_{cat} value for the mutants studied might vary based on an increasing/decreasing concentration of a specific structural form. Particularly given the unordered structure of WT and mutant proteins, there is significant scope for a broad equilibrium of conformational states and we explore this possibility below.

Identification of the active structural form. We have previously shown FR activity of α-syn in cells [19]. The cell based system has a distinct advantage over pure recombinant protein in that it is possible to

assess the localization of an active form of the protein. Ferrireductases are frequently membrane associated [26 27]. α-syn is also known to have a membrane association [28]. Therefore, we investigated the possibility that α-syn present in the membrane is more FR active than that present in the cytosol. A crude membrane extract was made from SH-SY5Y cells overexpressing α-syn. The level of α-syn present was compared between membrane and cytosolic fraction using western blot (Figure 4a). The majority of detectable protein was present in the cytosol. However, a small percentage was membrane associated. The quality of membrane isolation was verified using western blotting of the Na/K ATPase antiporter. The level of FR activity was then assessed for the membrane and cytosolic fractions and compared to activity in an unfractionated cell extract (total). Virtually all of the FR activity was present in the membrane rich fraction despite containing only a small fraction of the total cellular α-syn (Figure 4b). The implication is that the majority of FR activity present in α-syn overexpressing cells is located in the membrane fraction of SH-SY5Y cells. As a further step to verify that this activity was from α-syn we used a specific monoclonal antibody to immunoprecipitate (IP) α-syn from the membrane fractions. Ferriredactase activity was only associated with anti- α-syn IP material but not IP material when a control antibody was used (Suppl. Figure 3).

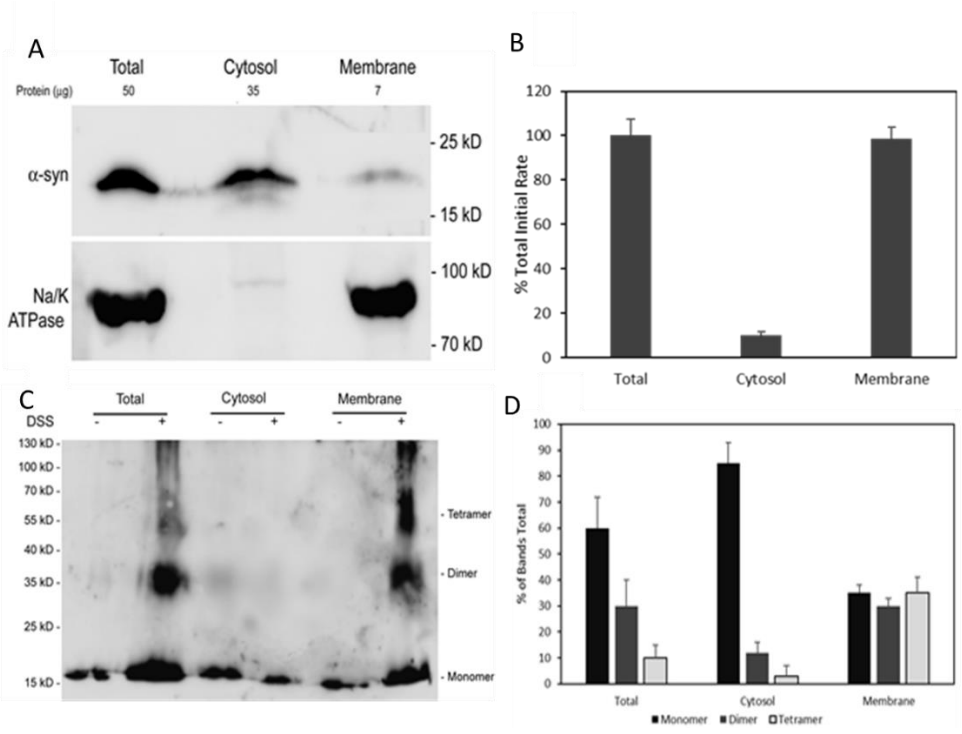

Figure 4. Identifying the structural form of FR active α-syn. **A**, Western blot of equivalent volumes of protein extracts prepared from SH-SY5Y cells overexpressing α-syn, separated into cytosolic and membrane fractions. The levels of α-syn and Na/K ATPase assessed by immunodetection. **B** The fractions from Panel A were then assayed for FR activity, quantified based on differences in the observed initial rate of ferrozine absorption change in the presence of 500 μM Fe(III). **C,** Western blot detecting cross linked α-syn from the SH-SY5Y fractions from Panel A. **D,** The relative amount of different α-syn oligomers from panel C were detected by densitometry. Data are the mean and s.e.m. for four experiments.

The localization of a small fraction of α-syn to the cell membrane and the association of this fraction with the majority of FR activity infers the structural identity of the most active species of α-syn. There has been suggestion that α-syn can be expressed in cells as a helical tetramer [11]. Identification of tetrameric α-syn can be achieved by cross-linking of the protein within cell extracts. Total, membrane

and cytosolic fractions of SH-SY5Y cell overexpressing α-syn were cross-linked and α-syn identified using western blot (Figure 4c). After fractionation, virtually all dimeric and tetrameric species of α-syn were present in the membrane fraction with almost solely monomeric protein in the cytosolic fraction. Also, in comparison to the total fraction, the level of tetrameric protein is clearly enriched. This strongly supports the notion that the active species is the tetrameric form of α-syn. Potentially the relatively small activity of the cytosolic fraction is attributable to the present of a minor amount of enzymatically active oligomeric α-syn present in the cytosol (Figure 4d).

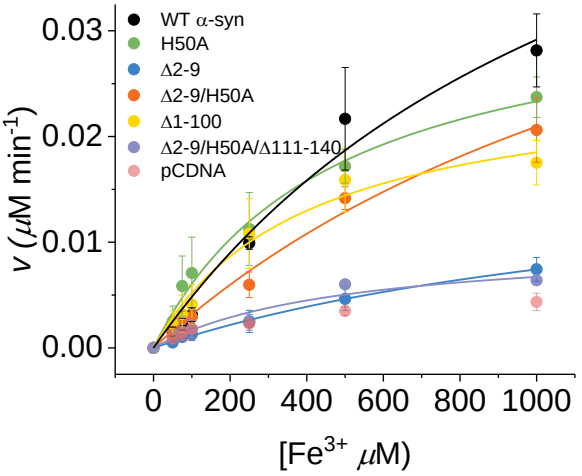

Figure 5. Steady-state kinetics of protein extract from α-syn expressing cell lines showing concentration dependencies for Fe(III). The membrane fractions from the cells were prepared as in Panel A. Protein concentrations were 250 μg/ml. The extracted kinetic parameters are given in Table 2.

Our finding that the major species showing ferriductase activity is associated with the membrane affords the opportunity to explore FR activity in the structural form found in the membrane, which we infer is a helical tetramer as described by others[11, 29]. To that end we have prepared protein extracts of the membrane fraction from cell lines overexpressing α-syn and a range of mutants. We assessed the kinetics of Δ2-9, Δ1-100, H50A, Δ2-9/H50A and Δ2-9/H50A/Δ111-140 to explore whether selected mutants have an additive effect. The observed activity with respect to Fe (III) concentration is shown in Figure 5

at essentially the same concentration of extracted total protein (250 μg/ml) and the extracted kinetic parameters in Table 2. The concentration range of Fe(III) we explore is necessarily more restricted compared to our recombinant protein studies because of the inherent capacity of high iron concentrations to cause cell components to precipitate. We therefore focus on the general trends that are apparent from the fitting shown in Figure 5. From the extracted kinetic parameters it is apparent that the variant enzymes show significant differences in the overall rate of turnover (asses by V_{max}, not k_{cat} since we do not know the precise enzyme concentration). Perhaps most importantly and consistent with our recombinant protein studies above, there is a clear difference in K_m, suggesting structurally different forms of the reactive complex geometry between the mutants. Notably, the triple mutant, Δ2-9/H50A/Δ111-140, has the lowest activity approaching that of the empty vector control cell extract (Table 2). Whilst we have fit the control vector to the Michaelis-Menten equation this is more for comparison since we do not expect these data to obey saturation behavior with respect to Fe (III) concentration and the fitting simply serves to illustrate the extremely small signal arising from potentially other membrane associated ferrireductases.

Table 2 . Extracted parameters from steady-state data fitting shown in Figure 5.

	V_{max} (μM/min)	K_m (mM)
α-syn	0.066 ± 0.02	1.28 ± 0.59
H50A	0.034 ± 0.003	0.46 ± 0.08
Δ2-9	0.018 ± 0.002	1.53 ± 0.19
Δ2-9, H50A	0.056 ± 0.014	1.68 ± 0.6
Δ1-100	0.026 ± 0.003	0.40 ± 0.1
Δ2-9, Δ111-140, H50A	0.01 ± 0.002	0.5 ± 0.2
pCDNA (negative control)	0.005 ± 0.001	255.9 ± 51

We wished to explore whether an artificial membrane environment could be used to drive the formation of helical α-syn and whether this is sufficient to induce FR activity. Recent studies have demonstrated that nano-discs – defined artificial membrane environments – can be used to induce α-syn to form helical multimers[30]. As these nano-discs had a protein scaffold they are not compatible with many protein biophysical techniques due to background 'noise' from the discs themselves. For this reason we used styrene-malate polymer scaffolds to make nanodiscs. These have been shown to be compatible with a range of optical biophysical measurements including CD and dynamic light scattering (DLS). We have incubated 5 μM recombinant α-syn in the presence of 50 μM lipid nanodiscs diluted from 7.5 mM nanodiscs prepared as described in materials and methods[31]. To assess α-syn incorporation and folding into the nanodiscs, we have monitored the far-UV CD spectra and the dynamic lights scattering (DLS) profile as shown in Figure 6A and 6B, respectively. We find that when α-syn is incubated with the nanodiscs, the far UV-CD data become consistent with a protein that is predominantly helical, showing negative ellipticity centered at ~205 and 222 nm. From Figure 6B, the DLS data show that the recombinant α-syn is initially at a high hydrodynamic diameter, indicative of a low *n* aggregated species. From Figure 6B the nanodiscs give a diameter ~ 10nm, consistent with previous reports of nanodiscs of this composition[32]. Incubation with the nanodiscs disaggregates this species, suggesting that the helical species incorporated into the nano-discs is not an aggregate or large multimer. On assaying the nanodisc - α-syn species with the FR assay described above, we found no detectable FR activity.

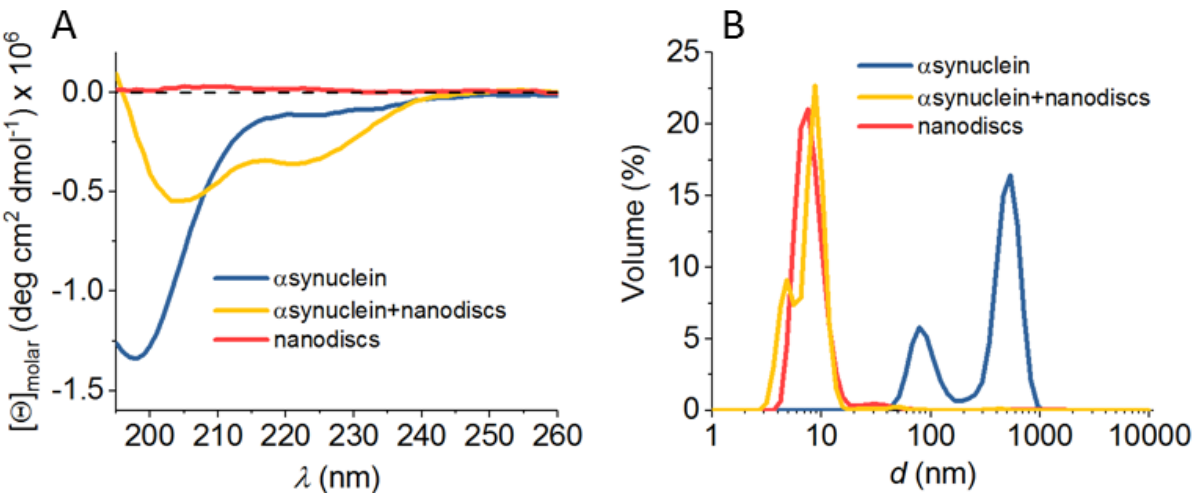

Figure 6. α-syn incorporation into nanodiscs. **A,** Far-UV CD spectra of recombinant free α-syn and bound to nanodiscs. **B,** DLS (volume) profiles of recombinant free α-syn and bound to nanodiscs.

Discussion

The function of many proteins associated with neurodegenerative diseases remains unresolved and frequently controversial. This is especially true for α-syn, a protein heavily implicated in a range of diseases collectively termed the synucleinopathies. The interest in the identification of a function for these proteins underlies the possibility that a loss or alteration of this function may play a causal role in the pathology. α-syn has been linked to altered metal metabolism. In PD there is especially a well-known change in iron metabolism[21, 22, 33]. Therefore, a function for α-syn related to iron is of great significance.

We previously provided evidence that α-syn acts as an FR[19]. An FR plays a vital role in a cell that requires Fe(II) as it allows the regeneration of this form of iron which is vital for many cellular activities. In dopaminergic neurons Fe(II) is required as a cofactor for tyrosine hydroxylase the key, rate limiting enzyme in the synthesis of dopamine. We showed that α-syn can increase cellular Fe(II) levels and that cells with increased α-syn have increased FR activity. Additionally, we showed using recombinant protein that α-syn exhibits FR activity when purified. In this report we provide a much expanded concentration range of substrates and explore the concentration-dependence of both NADH and Fe(III). These data allow greater insight in to the FR activity of α-syn, providing evidence of its *bona fide* enzymatic status, the role of substrate inhibition, and its dependence on NADH for activity. Most significantly we have provided evidence from cell studies that the active form of α-syn is a tetramer. This supports recent studies that have pointed out the structured (helical) tetrameric species as the more important subspecies *in vivo*[11, 34, 35].

Potentially, the α-syn ferrireductase activity is relatively low because only a small fraction of the protein exists in a conformation that is catalytically competent. This is highly likely as demonstrated by

the cell extract data where activity is associated with a subspecies isolated from membrane. It is important to note that when considering the recombinant protein that the amount of tetramer present is much less that the amount that can be detected in cells (around 2% of the total, data not shown). Alternatively, the activity could be relatively low because α-syn is primarily disordered in solution and so lacks a well-defined reactive geometry in the active site. This is less likely if the active species is a tetramer, as this has been shown to have high helical content [11, 35]. However, we note that the magnitude of K_m is independent of enzyme concentration and so even if a small fraction of the protein is catalytically active, the enzyme itself still displays a high K_m in relation to the cellular concentrations of both NADH and Fe^{3+}. Clearly however, local concentrations of substrates can be very much higher at the microscopic level.

From our recombinant protein studies we have found that the data fit to a model that includes substrate inhibition. The observation of substrate or product inhibition is relatively common and usually implies that the active site geometry can accommodate the substrate in more than one unique conformation, and at least some of these conformations are not catalytically competent. Typically, one observes the K_i value to be rather larger than the K_m since the binding of the substrate in the catalytically competent configuration is anticipated to be higher affinity than non-competent configurations. However, we find that for Fe (III) there is a 'turned-out' relationship for K_m and K_i, with the K_i being rather smaller than the K_m. A consequence of this unusual relationship is that wild-type α-syn exhibits a very sharp concentration dependence in activity as shown in Figure 2. We suggest that the relationship between K_m and K_i could be functionally important in governing the dose-response relationship of the intracellular pool of Fe(III)/ Fe(II). That is, the ferrireductase activity of α-syn will only become significant over a very narrow concentration range of available Fe(III).

Our data suggest that the enzymatically active form of α-syn is a membrane associated species, most likely to be the helical tetrameric species described recently[11]. However, we find that α-syn helicity is not itself sufficient to induce FR activity, with our artificial nanodisc - α-syn preparations showing no FR activity. Instead the FR activity is primarily associated with a structural form found in non-artificial cell membranes. These data argue that it is the precise quaternary structure of α-syn oligomers that define an active site compatible with FR activity. This finding suggests a possible mechanism by which α-syn acts as a ferrireductase. FR activity very commonly proceeds through a flavin intermediate, with hydride transfer from NAD(P)H, reducing the flavin and with subsequent reduction of Fe (III)[36]. Four-helix bundle architectures have been shown to bind flavin moieties and act as flavoenzymes[37] A realistic possibility for the FR activity of α-syn is therefore that the helical tetrameric assembly is capable of (likely weakly) binding flavin and using this species as a coenzyme to catalyse the reduction of Fe (III). This notion is satisfying since it would explain why we find the large majority of the FR activity associated with the membrane fraction where one expects the native helical tetramer to be prevalent. Moreover, this hypothesis would be consistent with the need of the helical oligomeric assembly to adopt a precise quaternary arrangement.

Kinetic assays with purified membrane protein fractions show saturation kinetics and the mutant proteins we have monitored show significant differences in both the overall turnover rate and the K_m. These data therefore are consistent with our recombinant protein assays in demonstrating that α-syn variants can affect the FR activity. The observed differences in overall turnover *and* K_m might point to difference in the active site architecture. That said we have shown previously that the Δ2-9/H50A mutant and deletions of the C-terminus alter membrane association [38]. The difference in the observed activity might therefore have an origin in an altered concentration of a catalytically competent structural form, i.e. membrane associated versus soluble. Another possibility is that the mutations alter the rate of tetramer formation.

A recent paper has identified the KTKEGF repeat regions through the protein sequence as being essential for tetramer formation. In contrast deletions of 10 amino acid residue stretches (eg. Δ2-10) had no effect on tetramer formation [34]. The implication is that changes in activity seen in our mutants are unlikely to be due to altered tetramer formation but instead are likely due to changes in membrane association. However, the key finding is these data support our notion that the FR active species is membrane associated and by inference the recently identified helical tetramer structural form.

The FR activity of α-syn is potentially important in understanding its pathological role, particularly since iron homeostasis is known to be important in PD. Herein we sought to explore steady-state kinetics of α-syn FR activity with a range of disease associated variants and exploring the nature of the catalytically active species. By exploring extended concentration ranges for the two substrates [NADH and Fe(III)] we found that turnover with NADH follows classical Michaelis-Menten kinetics, but with Fe(III) there is very significant substrate inhibition. Most importantly the kinetics of enzyme turnover, notably the inhibition and Michaelis constants, were significantly different with the disease variants. These data suggest that known disease variants of α-syn can 'tune' the FR activity. The observed rate of enzyme turnover are slow and we suggest this is because only a fraction of the enzyme is in a catalytically competent conformation, lacks a necessary cofactor or both. Whole cell assays point to the FR active α-syn being a membrane associated tetrameric species, which we suggest is the recently identified helical tetrameric form. By using artificial membrane constructs (nanodiscs) we found that inducing α-syn to form a helical conformation is not itself sufficient to induce FR activity, suggesting that the absolute precision of the quaternary arrangement of helical α-syn monomers is necessary to define the catalytically active species. We go on to suggest that a rational mechanism for the FR activity of α-syn might be the binding of a flavin coenzyme by the helical tetrameric α-syn, which then mediates the electron transfer from NADH to Fe(III) as in other ferrireductases.

Acknowledgments. The authors thank the UK charities BRACE and Alzheimer's Research UK (ARUK-PG2012-1) for funding the project. We thank Mr Morgan Roberts for technical assistance in preparation of the nanodiscs.

References

[1] George, J. M. (2002) The synucleins, *Genome Biol 3*, REVIEWS3002.

[2] Clayton, D. F., and George, J. M. (1998) The synucleins: a family of proteins involved in synaptic function, plasticity, neurodegeneration and disease, *Trends Neurosci 21*, 249-254.

[3] Burke, R. E. (2004) Recent advances in research on Parkinson disease: synuclein and parkin, *Neurologist 10*, 75-81.

[4] Goedert, M. (2001) Parkinson's disease and other alpha-synucleinopathies, *Clin Chem Lab Med 39*, 308-312.

[5] Jakes, R., Spillantini, M. G., and Goedert, M. (1994) Identification of two distinct synucleins from human brain, *FEBS Lett 345*, 27-32.

[6] Spillantini, M. G., Schmidt, M. L., Lee, V. M., Trojanowski, J. Q., Jakes, R., and Goedert, M. (1997) Alpha-synuclein in Lewy bodies, *Nature 388*, 839-840.

[7] Bussell, R., Jr., and Eliezer, D. (2003) A structural and functional role for 11-mer repeats in alpha-synuclein and other exchangeable lipid binding proteins, *J Mol Biol 329*, 763-778.

[8] Jao, C. C., Der-Sarkissian, A., Chen, J., and Langen, R. (2004) Structure of membrane-bound alpha-synuclein studied by site-directed spin labeling, *Proc Natl Acad Sci U S A 101*, 8331-8336.

[9] Jo, E., Fuller, N., Rand, R. P., St George-Hyslop, P., and Fraser, P. E. (2002) Defective membrane interactions of familial Parkinson's disease mutant A30P alpha-synuclein, *J Mol Biol 315*, 799-807.

[10] Vamvaca, K., Volles, M. J., and Lansbury, P. T., Jr. (2009) The first N-terminal amino acids of alpha-synuclein are essential for alpha-helical structure formation in vitro and membrane binding in yeast, *J Mol Biol 389*, 413-424.

[11] Bartels, T., Choi, J. G., and Selkoe, D. J. (2011) alpha-Synuclein occurs physiologically as a helically folded tetramer that resists aggregation, *Nature 477*, 107-110.

[12] Abeliovich, A., Schmitz, Y., Farinas, I., Choi-Lundberg, D., Ho, W. H., Castillo, P. E., Shinsky, N., Verdugo, J. M., Armanini, M., Ryan, A., Hynes, M., Phillips, H., Sulzer, D., and Rosenthal, A. (2000) Mice lacking alpha-synuclein display functional deficits in the nigrostriatal dopamine system, *Neuron 25*, 239-252.

[13] Pena-Oliver, Y., Buchman, V. L., Dalley, J. W., Robbins, T. W., Schumann, G., Ripley, T. L., King, S. L., and Stephens, D. N. (2012) Deletion of alpha-synuclein decreases impulsivity in mice, *Genes Brain Behav 11*, 137-146.

[14] Sidhu, A., Wersinger, C., and Vernier, P. (2004) Does alpha-synuclein modulate dopaminergic synaptic content and tone at the synapse?, *FASEB J 18*, 637-647.

[15] Burre, J., Sharma, M., Tsetsenis, T., Buchman, V., Etherton, M. R., and Sudhof, T. C. (2010) Alpha-synuclein promotes SNARE-complex assembly in vivo and in vitro, *Science 329*, 1663-1667.

[16] Boassa, D., Berlanga, M. L., Yang, M. A., Terada, M., Hu, J., Bushong, E. A., Hwang, M., Masliah, E., George, J. M., and Ellisman, M. H. (2013) Mapping the subcellular distribution of alpha-synuclein in neurons using genetically encoded probes for correlated light and electron microscopy: implications for Parkinson's disease pathogenesis, *J Neurosci 33*, 2605-2615.

[17] Kontopoulos, E., Parvin, J. D., and Feany, M. B. (2006) Alpha-synuclein acts in the nucleus to inhibit histone acetylation and promote neurotoxicity, *Hum Mol Genet 15*, 3012-3023.

[18] Ellis, C. E., Murphy, E. J., Mitchell, D. C., Golovko, M. Y., Scaglia, F., Barcelo-Coblijn, G. C., and Nussbaum, R. L. (2005) Mitochondrial lipid abnormality and electron transport chain impairment in mice lacking alpha-synuclein, *Mol Cell Biol 25*, 10190-10201.

[19] Davies, P., Moualla, D., and Brown, D. R. (2011) Alpha-synuclein is a cellular ferrireductase, *PLoS One 6*, e15814.

[20] Kaushik, P., Gorin, F., and Vali, S. (2007) Dynamics of tyrosine hydroxylase mediated regulation of dopamine synthesis, *J Comput Neurosci 22*, 147-160.
[21] Dexter, D. T., Wells, F. R., Agid, F., Agid, Y., Lees, A. J., Jenner, P., and Marsden, C. D. (1987) Increased nigral iron content in postmortem parkinsonian brain, *Lancet 2*, 1219-1220.
[22] Dexter, D. T., Wells, F. R., Lees, A. J., Agid, F., Agid, Y., Jenner, P., and Marsden, C. D. (1989) Increased nigral iron content and alterations in other metal ions occurring in brain in Parkinson's disease, *J Neurochem 52*, 1830-1836.
[23] Davies, P., Wang, X., Sarell, C. J., Drewett, A., Marken, F., Viles, J. H., and Brown, D. R. (2011) The synucleins are a family of redox-active copper binding proteins, *Biochemistry 50*, 37-47.
[24] LiCata, V. J., and Allewell, N. M. (1997) Is substrate inhibition a consequence of allostery in aspartate transcarbamylase?, *Biophys Chem 64*, 225-234.
[25] Binolfi, A., Rasia, R. M., Bertoncini, C. W., Ceolin, M., Zweckstetter, M., Griesinger, C., Jovin, T. M., and Fernandez, C. O. (2006) Interaction of alpha-synuclein with divalent metal ions reveals key differences: a link between structure, binding specificity and fibrillation enhancement, *J Am Chem Soc 128*, 9893-9901.
[26] Ohgami, R. S., Campagna, D. R., McDonald, A., and Fleming, M. D. (2006) The Steap proteins are metalloreductases, *Blood 108*, 1388-1394.
[27] Pantopoulos, K., Porwal, S. K., Tartakoff, A., and Devireddy, L. (2012) Mechanisms of mammalian iron homeostasis, *Biochemistry 51*, 5705-5724.
[28] McLean, P. J., Kawamata, H., Ribich, S., and Hyman, B. T. (2000) Membrane association and protein conformation of alpha-synuclein in intact neurons. Effect of Parkinson's disease-linked mutations, *J Biol Chem 275*, 8812-8816.
[29] Dettmer, U., Newman, A. J., Luth, E. S., Bartels, T., and Selkoe, D. (2013) In vivo cross-linking reveals principally oligomeric forms of alpha-synuclein and beta-synuclein in neurons and non-neural cells, *J Biol Chem 288*, 6371-6385.
[30] Eichmann, C., Campioni, S., Kowal, J., Maslennikov, I., Gerez, J., Liu, X., Verasdonck, J., Nespovitaya, N., Choe, S., Meier, B. H., Picotti, P., Rizo, J., Stahlberg, H., and Riek, R. (2016) Preparation and characterization of stable alpha-synuclein lipoprotein particles, *J Biol Chem 291*, 8516-8527.
[31] Lee, S. C., Knowles, T. J., Postis, V. L., Jamshad, M., Parslow, R. A., Lin, Y. P., Goldman, A., Sridhar, P., Overduin, M., Muench, S. P., and Dafforn, T. R. (2016) A method for detergent-free isolation of membrane proteins in their local lipid environment, *Nature protocols 11*, 1149-1162.
[32] Zhang, R., Sahu, I. D., Liu, L., Osatuke, A., Comer, R. G., Dabney-Smith, C., and Lorigan, G. A. (2015) Characterizing the structure of lipodisq nanoparticles for membrane protein spectroscopic studies, *Biochim Biophys Acta 1848*, 329-333.
[33] Dexter, D. T., Carayon, A., Javoy-Agid, F., Agid, Y., Wells, F. R., Daniel, S. E., Lees, A. J., Jenner, P., and Marsden, C. D. (1991) Alterations in the levels of iron, ferritin and other trace metals in Parkinson's disease and other neurodegenerative diseases affecting the basal ganglia, *Brain 114*, 1953-1975.
[34] Dettmer, U., Newman, A. J., von Saucken, V. E., Bartels, T., and Selkoe, D. (2015) KTKEGV repeat motifs are key mediators of normal alpha-synuclein tetramerization: Their mutation causes excess monomers and neurotoxicity, *Proc Natl Acad Sci U S A 112*, 9596-9601.
[35] Wang, W., Perovic, I., Chittuluru, J., Kaganovich, A., Nguyen, L. T., Liao, J., Auclair, J. R., Johnson, D., Landeru, A., Simorellis, A. K., Ju, S., Cookson, M. R., Asturias, F. J., Agar, J. N., Webb, B. N., Kang, C., Ringe, D., Petsko, G. A., Pochapsky, T. C., and Hoang, Q. Q. (2011) A soluble alpha-synuclein construct forms a dynamic tetramer, *Proc Natl Acad Sci U S A 108*, 17797-17802.

[36] Schroder, I., Johnson, E., and de Vries, S. (2003) Microbial ferric iron reductases, *FEMS microbiology reviews 27*, 427-447.

[37] Tomizaki, K., Tsunekawa, Y., Akisada, H., Miharac, H., and Nishino, N. (2000) Design and characterization of flavoenzyme models in the course of chemical evolution of four-α-helix bundle polypeptides *J. Chem. Soc. Perkin Trans. 2*, 813-822.

[38] Wang, X., Moualla, D., Wright, J. A., and Brown, D. R. (2010) Copper binding regulates intracellular alpha-synuclein localisation, aggregation and toxicity, *J Neurochem 113*, 704-714.